AMERICAN SOCIETY FOR MICROBIOLOGY | mBio®

RESEARCH ARTICLE

Role of the Antigen Capture Pathway in the Induction of a Neutralizing Antibody Response to Anthrax Protective Antigen

Anita Verma,[a] Miriam M. Ngundi,[a] Gregory A. Price,[a] Kazuyo Takeda,[a] James Yu,[a] Drusilla L. Burns[a]

[a]Center for Biologics Evaluation and Research, Food and Drug Administration, Silver Spring, Maryland, USA

ABSTRACT Toxin neutralizing antibodies represent the major mode of protective immunity against a number of toxin-mediated bacterial diseases, including anthrax; however, the cellular mechanisms that lead to optimal neutralizing antibody responses remain ill defined. Here we show that the cellular binding pathway of anthrax protective antigen (PA), the binding component of anthrax toxin, determines the toxin neutralizing antibody response to this antigen. PA, which binds cellular receptors and efficiently enters antigen-presenting cells by receptor-mediated endocytosis, was found to elicit robust anti-PA IgG and toxin neutralizing antibody responses. In contrast, a receptor binding-deficient mutant of PA, which does not bind receptors and only inefficiently enters antigen-presenting cells by macropinocytosis, elicited very poor antibody responses. A chimeric protein consisting of the receptor binding-deficient PA mutant tethered to the binding subunit of cholera toxin, which efficiently enters cells using the cholera toxin receptor rather than the PA receptor, elicited an anti-PA IgG antibody response similar to that elicited by wild-type PA; however, the chimeric protein elicited a poor toxin neutralizing antibody response. Taken together, our results demonstrate that the antigen capture pathway can dictate the magnitudes of the total IgG and toxin neutralizing antibody responses to PA as well as the ratio of the two responses.

IMPORTANCE Neutralizing antibodies provide protection against a number of toxin-mediated bacterial diseases by inhibiting toxin action. Therefore, many bacterial vaccines are designed to induce a toxin neutralizing antibody response. We have used protective antigen (PA), the binding component of anthrax toxin, as a model antigen to investigate immune mechanisms important for the induction of robust toxin neutralizing antibody responses. We found that the pathway used by antigen-presenting cells to capture PA dictates the robustness of the neutralizing antibody response to this antigen. These results provide new insights into immune mechanisms that play an important role in the induction of toxin neutralizing antibody responses and may be useful in the design of new vaccines against toxin-mediated bacterial diseases.

KEYWORDS anthrax protective antigen, antigen capture, neutralizing antibodies, toxin neutralization

Vaccines against toxin-mediated bacterial diseases, such as diphtheria, tetanus, and anthrax, protect by eliciting robust toxin neutralizing antibody responses. The major antigen of each of these vaccines is an inactivated form of the relevant toxin. To elicit a robust humoral response, the vaccine antigen is captured by antigen-presenting cells (APCs) which induce antigen-specific T and B cell responses (1). For presentation to T cells, APCs internalize and process antigens to present antigen-derived peptides on major histocompatibility complexes (MHC) which results in the T cell help needed for robust antibody responses. The mechanism by which antigen is presented by APCs to B cells is less well defined. For induction of toxin neutralizing antibodies, the B cells that

Received 26 January 2018 **Accepted** 29 January 2018 **Published** 27 February 2018

Citation Verma A, Ngundi MM, Price GA, Takeda K, Yu J, Burns DL. 2018. Role of the antigen capture pathway in the induction of a neutralizing antibody response to anthrax protective antigen. mBio 9:e00209-18. https://doi.org/10.1128/mBio.00209-18.

Editor Jimmy D. Ballard, University of Oklahoma Health Sciences Center

Address correspondence to Drusilla L. Burns, drusilla.burns@fda.hhs.gov.

This article is a direct contribution from a Fellow of the American Academy of Microbiology. Solicited external reviewers: Erik Hewlett, University of Virginia School of Medicine; Steven Blanke, Univ. of Illinois Urbana.

are stimulated must be capable of producing antibodies that recognize and inactivate the native form of the toxin. Thus, for induction of toxin neutralizing antibodies, APCs would need to retain epitopes in their native conformation for display to the surface immunoglobulin receptor of B cells (2, 3). Studies have suggested that certain APCs, such as dendritic cells, can have both degradative and nondegradative antigen uptake pathways to facilitate presentation to T cells and B cells, respectively (3). The features of antigen uptake pathways that are critical for induction of optimal toxin neutralizing antibody responses have been poorly characterized. In order to begin to investigate the role that antigen uptake pathways play in induction of toxin neutralizing antibody responses, we examined the role that the uptake pathway of anthrax protective antigen (PA), the binding component of anthrax toxin, plays in the antibody response to this protein. PA was chosen for this study because the cellular binding and internalization pathway of PA has been well defined (4, 5) and its uptake pathway can be altered by genetic manipulation.

Anthrax toxin consists of PA and two catalytically active components, lethal factor (LF) and edema factor (EF). Interaction of PA with LF results in the formation of lethal toxin (LT); interaction of PA with EF results in the formation of edema toxin (ET). PA (83 kDa) initiates anthrax toxin action by interacting with specific target cell receptors. Two cellular proteins have been shown to be capable of serving as a receptor for PA, capillary morphogenesis protein 2 (CMG2) and tumor endothelial marker 8 (TEM8), with CMG2 being the major receptor (6). After binding to its cell receptor, PA is cleaved by cell surface proteases to PA63 (63 kDa) and PA20 (20 kDa). The receptor-bound PA63 oligomerizes to form a heptamer which then binds LF and/or EF. The receptor-bound toxin complex is then endocytosed where the low pH of the endosome induces the PA oligomer to form a pore in the membrane which is capable of translocating the catalytic units of the toxin across the membrane (7). Within the early endosome, the membrane-bound toxin complex is preferentially incorporated into intraluminal vesicles of the endosome rather than the limiting membrane. Ultimately, the toxin-containing intraluminal vesicles are trafficked to late endosomes (8) for subsequent release of the catalytic units into the cell cytoplasm.

PA is immunogenic and elicits toxin neutralizing antibodies that have been shown to correlate with protection against anthrax disease (9–11). In this study, we found that the ability of PA to bind to its cellular receptor had a striking effect on its capability to elicit a toxin neutralizing antibody response. Generation of an optimal neutralizing response was dependent on the PA-specific binding/internalization pathway, since cellular uptake of PA by an alternate binding/internalization pathway, the cholera toxin uptake pathway, resulted in a suboptimal neutralizing response. This work demonstrates the importance of the PA receptor-specific binding pathway in eliciting a neutralizing antibody response to PA and demonstrates that antigen uptake pathways can dictate the robustness of the neutralizing antibody response.

RESULTS

Role of receptor binding in antibody response to PA. We were led to examine the role that receptor binding plays in the antibody response to PA, since in our previous work, we demonstrated that spontaneous deamidation of asparagine residues in PA is associated with a loss in the ability of the antigen to elicit toxin neutralizing antibodies (12), and as shown by others, deamidated PA exhibits reduced binding to cells (13). Thus, we reasoned that reduced binding of PA to its receptor might contribute to the loss of immunogenicity. To test the possibility that binding of PA to its receptor plays a role in its ability to elicit an antibody response, we utilized a receptor binding-deficient (RBD) form of PA that does not bind to its cellular receptors due to mutations (N682A and D683A) in its receptor-binding region (14, 15). We confirmed the lack of ability of this double mutant PA to bind to cells by incubating J774A.1 cells with either wild-type PA or the RBD mutant PA at 4°C, washing away unbound PA protein, and subjecting the cell lysates to immunoblot analysis using a PA-specific antibody to visualize any PA protein that had bound to the cells. While

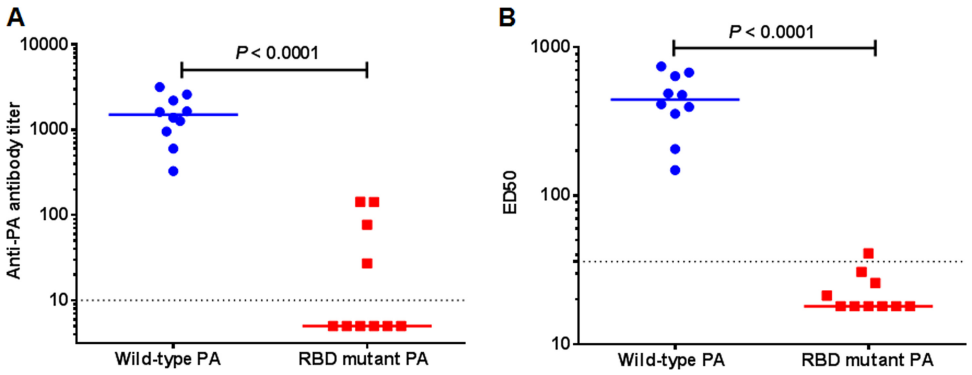

FIG 1 Antibody titers of mice immunized with wild-type PA and RBD mutant PA. Two groups (10 mice in each group) were immunized with either wild-type PA or RBD mutant PA (15 μg of antigen/mouse). Twenty-eight days postimmunization, the mice were bled, and serum samples were analyzed by ELISA or the toxin neutralizing antibody assay as described in Materials and Methods. (A) Anti-PA IgG antibody titers for mice as determined by ELISA. (B) Toxin neutralizing antibody titer (expressed as ED_{50}) for mice. Each symbol represents the value for an individual mouse. The horizontal line represents the median for the group of mice. The Mann-Whitney test was used to determine statistical significance, and the *P* value is indicated. The dotted line represents the limit of quantitation of the assay. This figure shows the results of one experiment and is representative of three independent immunization experiments.

bound wild-type PA was readily detected, we were unable to visualize any binding of the RBD mutant PA to the cells (data not shown). We then compared the ability of the wild-type PA to induce an antibody response in mice to that of the RBD mutant PA. Groups of mice were immunized with either wild-type or RBD mutant PA. Individual serum samples were analyzed for total anti-PA IgG antibodies utilizing an enzyme-linked immunosorbent assay (ELISA) and for toxin neutralizing antibodies utilizing a cell culture assay that assesses antibody-mediated neutralization of lethal toxin (LF plus PA). As shown in Fig. 1A, total anti-PA IgG antibody titers of mice immunized with wild-type PA were dramatically higher than those of mice immunized with RBD mutant PA. Toxin neutralizing titers of mice immunized with wild-type PA were also strikingly higher than those of mice immunized with RBD mutant PA (Fig. 1B). These data suggest that receptor binding of PA results in the induction of a robust total IgG antibody response as well as a toxin neutralizing antibody response.

To ensure that the poor antibody response to RBD mutant PA was not due to differences in tertiary structures of the wild-type and RBD mutant PA proteins, we measured the melting temperatures (T_m) of the two proteins, since thermal stability of a protein reflects its tertiary structure. The T_m of both the wild-type and RBD mutant PA was 47°C, indicative of similar tertiary structures. We also examined the protease susceptibility of the two proteins. Wild-type PA (83 kDa) is known to be cleaved into two fragments of 63 kDa and 20 kDa by trypsin and into two fragments of 47 kDa and 37 kDa by chymotrypsin (16). We found that identical proteolytic patterns were generated when wild-type PA and RBD mutant PA were subjected to treatment with either trypsin or chymotrypsin (data not shown), also indicative of similar tertiary structures. We also conducted ELISAs where we coated the wells on the plates with either wild-type PA or the RBD mutant PA and then examined the ELISA titers of sera from mice immunized with wild-type PA using the two different sets of plates. We found no significant difference in the titers of the sera between the two sets of plates (data not shown).

To further demonstrate the structural integrity of the RBD mutant PA and to ensure that the poor neutralizing antibody response to RBD mutant PA was not due to loss of immunodominant epitopes involving amino acids at positions 682 and 683 which were altered in the RBD mutant PA, we depleted a PA-specific immune serum pool by adsorbing the serum with either wild-type PA or the RBD mutant PA and then assayed the depleted serum for toxin neutralizing antibodies. If the RBD mutant PA was missing critical immunodominant epitopes or if its structure was different from that of wild-type

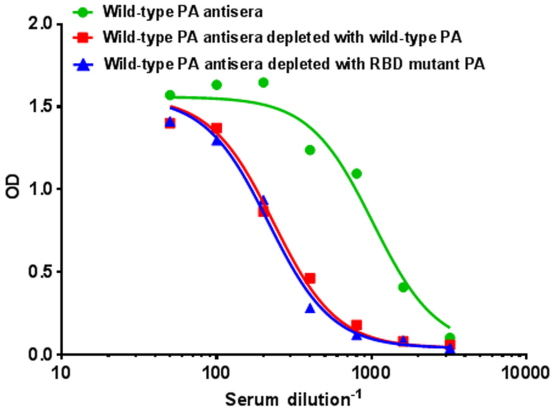

FIG 2 Toxin neutralizing antibody depletion analysis. Pooled sera from mice immunized with wild-type PA was adsorbed with either wild-type PA or RBD mutant PA conjugated to magnetic beads as described in Materials and Methods. After depletion, the toxin neutralizing antibody assay was performed to assess the extent of neutralizing antibody depletion by the individual PA proteins. Absorbance (optical density [OD]) measured in the toxin neutralizing antibody assay is plotted against the dilution of antiserum.

PA, we would expect that the RBD mutant PA would not be capable of binding to and depleting the neutralizing antibodies present in the immune serum to an extent comparable to that of wild-type PA. However, we found that the RBD mutant PA was as potent as wild-type PA in its ability to deplete neutralizing antibodies from the PA-specific immune serum (Fig. 2). These results suggest that the amino acid changes (N682A and D683A) in RBD mutant PA did not result in loss of an epitope(s) that is important for the generation of toxin neutralizing antibodies and provide further evidence that the structure of the RBD mutant PA did not differ from that of wild-type PA.

Internalization of PA proteins by DC 2.4 cells. Our data demonstrating that wild-type PA elicits a much more robust antibody response than that induced by the RBD mutant PA which does not bind to receptor suggest that the binding of PA to its receptor and possibly its subsequent internalization influence the antibody response following PA immunization. In order to visualize and compare the internalization of wild-type PA and RBD mutant PA into APCs, we utilized the DC 2.4 murine dendritic cell line as a model APC. DC 2.4 cells were incubated with either wild-type PA labeled with DyLight 594 (red) or RBD mutant PA labeled with DyLight 488 (green). After 30 min of incubation at 37°C, the cells were processed for confocal microscopy. As shown in Fig. 3A, labeled wild-type PA (red) exhibited a staining pattern along cell boundaries, consistent with binding of labeled wild-type PA to the receptors present on the cell surface, as well as staining within the cell indicative of internalized protein. In comparison, very little labeled RBD mutant PA (green) could be observed, and no distinct labeling of the cell surface was seen, highlighting the inability of the RBD mutant PA to bind cell surface receptors. Some RBD mutant PA did enter the cells although at greatly reduced levels compared to wild-type PA. Entry of RBD mutant PA into DC 2.4 cells was better visualized when 20 times the amount of RBD mutant PA was used. Figure 3B shows a confocal image of DC 2.4 cells that were incubated with wild-type PA at 5 μg/ml and the RBD mutant PA at 100 μg/ml. While binding of wild-type PA to the cell surface (red) can be clearly seen, no cell surface binding of the RBD mutant PA is evident (green). The merged image highlights binding of wild-type PA and the lack of binding of the RBD mutant PA to the cell surface. Moreover, this image clearly shows that both PA proteins were internalized.

We further studied cellular internalization of both wild-type PA and the RBD mutant PA by incubating DC 2.4 cells with either wild-type PA (10 μg/ml) or the RBD mutant PA (100 μg/ml) for 90 min at 37°C. The cells were then treated with acid to remove PA bound to the cell surface. Cell lysates were prepared, and internalized wild-type PA or RBD mutant PA was visualized by immunoblot analysis. In this experiment, levels of RBD

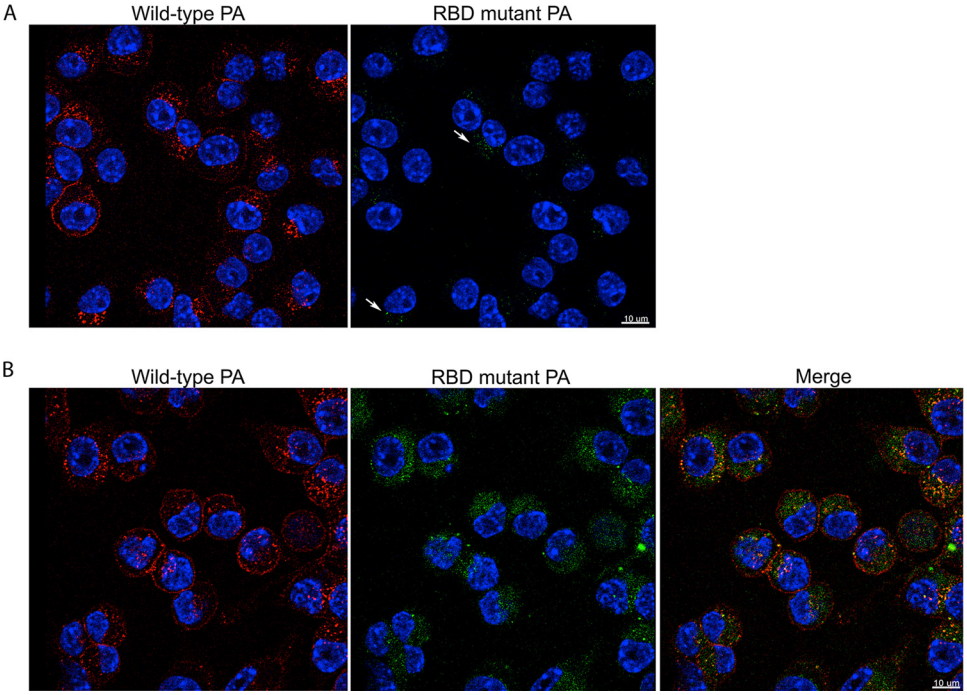

FIG 3 Visualization of internalization of wild-type PA and RBD mutant PA into DC 2.4 cells by confocal microscopy. (A and B) DC 2.4 cells that had been incubated with fluorescently labeled wild-type PA (red) or RBD mutant PA (green) at concentrations of 5 μg/ml each (A) or concentrations of 5 μg/ml for wild-type PA and 100 μg/ml for RBD mutant PA (B) were visualized by confocal microscopy. Cell nuclei were counterstained with DAPI (blue). White arrows in panel A indicate internalized RBD mutant PA.

mutant PA 10 times higher than the level of wild-type PA were used in order to allow visualization of internalized RBD mutant PA by immunoblotting. As shown in Fig. 4A (lane 1) and Fig. 4B (lane 1), both internalized wild-type PA and RBD mutant PA are seen primarily as either PA63 or a higher-molecular-weight form of PA63 that is resistant to sodium dodecyl sulfate (SDS) denaturation that was previously identified as the oligomeric pore form of PA (5). Smaller amounts of PA83 are present. Thus, both the internalized wild-type PA and RBD mutant PA can be cleaved by cellular proteases to the 63-kDa species, which can then form oligomeric pores within the cells. The finding that the RBD mutant PA was correctly cleaved to the 63-kDa species and was capable

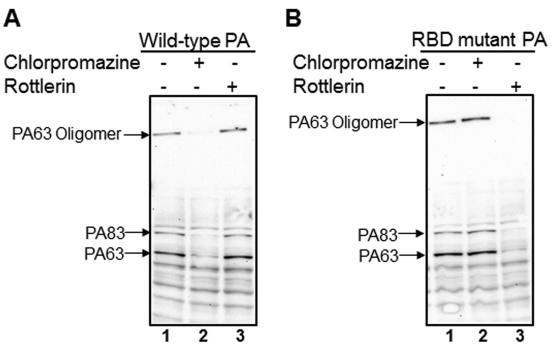

FIG 4 Immunoblot analysis of the internalization of wild-type PA and RBD mutant PA by DC 2.4 cells. (A and B) DC 2.4 cells were incubated with wild-type PA (10 μg/ml) (A) or RBD mutant PA (100 μg/ml) (B) for 90 min at 37°C in the presence (+) or absence (−) of chlorpromazine or rottlerin. After the cells were incubated, they were washed, lysed, and subjected to immunoblotting as described in Materials and Methods. Lane 1, no inhibitors; lane 2, inhibition by chlorpromazine; lane 3, inhibition by rottlerin. The positions of PA83, PA63, and PA63 oligomers are shown to the left of the blots.

of forming SDS-resistant pores further confirms that the RBD mutant PA retains the structure of wild-type PA.

In order to identify the routes of cellular entry of wild-type PA and RBD mutant PA, we used inhibitors of endocytic pathways. We used chlorpromazine which specifically inhibits clathrin-dependent receptor-mediated endocytosis (17) and rottlerin which specifically inhibits the nonspecific fluid-phase internalization pathway known as macropinocytosis (18). As shown in Fig. 4A (lanes 2 and 3), internalization of wild-type PA is inhibited by chlorpromazine but not by rottlerin. In contrast, internalization of the RBD mutant PA into DC 2.4 cells is inhibited by rottlerin, but not by chlorpromazine (Fig. 4B, lanes 2 and 3). These results demonstrate that while wild-type PA enters DC 2.4 cells by receptor-mediated endocytosis, the RBD mutant PA enters the cells by nonspecific, fluid-phase macropinocytosis. The efficiency of entry of the RBD mutant PA is much less than that of wild-type PA, since 10 times more RBD mutant PA was used in this experiment than wild-type PA, yet approximately the same amount of wild-type PA and RBD mutant PA appeared to be internalized, which is consistent with the low efficiency of internalization of the RBD mutant PA observed by confocal microscopy (Fig. 3A).

Effect of altering the route of receptor-mediated entry on the immunogenicity of PA. A low efficiency of binding of the RBD mutant PA by APCs could explain the low levels of total anti-PA IgG and toxin neutralizing antibody elicited by immunization. However, when we immunized mice with 15 μg/mouse of wild-type PA and 150 μg/mouse of RBD mutant PA, antibody titers elicited by the RBD mutant PA (both total anti-PA IgG and toxin neutralizing antibody titers) remained significantly lower than those elicited by wild-type PA (data not shown). In order to investigate whether the efficiency of binding of the RBD mutant PA to APCs is the sole cause of the low antibody response to RBD mutant PA or whether the specific binding/internalization pathway used by an antigen could also play a role, we constructed an RBD mutant PA chimeric protein which could efficiently bind to and enter cells but via a different receptor-mediated entry pathway than that taken by wild-type PA. The chimeric protein that we constructed consisted of the RBD mutant PA fused to the A2 peptide of cholera toxin. Coexpression of this fusion protein with the B subunit of cholera toxin (CTB) results in a chimeric protein consisting of the RBD mutant PA noncovalently tethered to the CTB pentamer by the A2 peptide (RBD PA-A2-CTB). Electrophoretic analysis of the purified RBD PA-A2-CTB chimeric protein confirmed this composition (Fig. 5A and B).

CTB enters cells by binding to ganglioside GM_1 on the cell surface and then follows an internalization pathway distinct from the pathway utilized by PA (19, 20). The RBD PA-A2-CTB chimeric protein would be expected to utilize the cholera toxin entry pathway. In order to confirm that the RBD PA-A2-CTB chimera was capable of binding to and entering cells, we visualized internalization of the RBD PA-A2-CTB chimera by DC 2.4 cells, which we used as a model APC, and compared the efficiency of internalization to that of wild-type PA. As shown in Fig. 5C (lane 2), the RBD PA-A2-CTB chimera readily entered DC 2.4 cells. In fact, the efficiency of internalization was much greater than that observed when an equimolar amount of wild-type PA (Fig. 5C, lane 1) was used. It is noteworthy that RAW 264.7 cells, a murine macrophage-like cell, also exhibited the very efficient uptake of the RBD PA-A2-CTB chimera that we observed with the DC 2.4 cells (data not shown). The protein pattern observed for the chimeric protein internalized by DC 2.4 cells was similar to that of wild-type PA in that the RBD-A2 portion of the chimera was primarily found as the cleaved PA63 analog and an SDS-resistant oligomeric pore, with smaller amounts of the uncleaved PA83 analog observed. To confirm that the RBD PA-A2-CTB chimera was entering cells via the cholera toxin internalization pathway, we constructed a similar chimera using a mutant CTB (CTB G33D) which has a mutation at position 33, rendering the protein incapable of binding to the cholera toxin receptor (21). As shown in Fig. 5C (lane 3), this mutant RBD PA-A2-CTB(G33D) chimera was not internalized by DC 2.4 cells. Thus, the RBD PA-A2-CTB chimera efficiently bound to and entered cells via the cholera toxin receptor. It is noteworthy

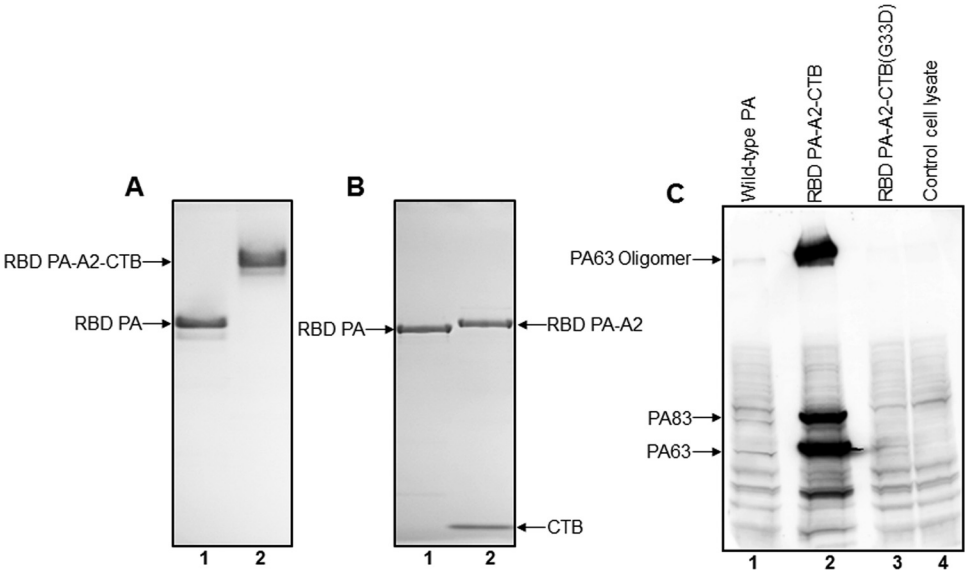

FIG 5 Characterization of RBD PA-A2-CTB chimera and its internalization by DC 2.4 cells. (A) Native gel electrophoresis of the purified chimera. Lane 1, RBD mutant PA; lane 2, RBD PA-A2-CTB chimera. (B) SDS-polyacrylamide gel electrophoresis of the purified chimera. Lane 1, RBD mutant PA (83 kDa); lane 2, RBD PA-A2-CTB chimera comprising the RBD PA-A2 fusion subunit (86.5 kDa) and CTB subunit (11.7 kDa). (C) Internalization by DC 2.4 cells. DC 2.4 cells were incubated with equimolar amounts of wild-type PA (10 μg/ml) (lane 1), the RBD PA-A2-CTB chimera (17.5 μg/ml) (lane 2), or RBD PA-A2-CTB(G33D) (17.5 μg/ml) (lane 3) for 90 min at 37°C. After the cells were incubated, they were washed, lysed, and subjected to immunoblotting as described in Materials and Methods. The positions of PA83, PA63, and PA63 oligomers are indicated to the left of the blots.

that the RBD portion of the RBD PA-A2-CTB chimera was properly cleaved to a species analogous to PA63 which could form oligomeric pore structures. These results confirm that the RBD portion of the chimera retains a structure similar to that of wild-type PA.

We next assessed the immunogenicity of the RBD PA-A2-CTB chimeric protein and compared it to that of wild-type PA. Groups of 10 mice were immunized with either wild-type PA or the RBD PA-A2-CTB chimera. Immunogenicity elicited by the RBD PA-A2-CTB(G33D) chimera was also assessed. As shown in Fig. 6A, the total anti-PA IgG antibody response elicited by RBD PA-A2-CTB, as measured by ELISA, was not statistically different from that elicited by wild-type PA. However, the neutralizing antibody response elicited by the RBD PA-A2-CTB chimera was approximately sevenfold lower than that elicited by wild-type PA (Fig. 6B). Neither RBD PA-A2-CTB(G33D) (Fig. 6A and B) nor RBD plus CTB (data not shown) elicited a significant total anti-PA IgG or toxin neutralizing antibody response. Our finding that RBD PA-A2-CTB elicited higher IgG antibody titers than those elicited by the cholera toxin receptor binding-deficient chimera, RBD PA-A2-CTB(G33D), demonstrates that the RBD PA-A2-CTB chimera is binding to cells through the cholera toxin receptor. The enhanced IgG response that we observed with the receptor binding-competent chimera is consistent with previous work that has showed that cholera toxin-antigen chimeras can improve the immune response to an antigen compared with admixtures of the antigen with CTB (22).

Taken together, these data indicate that the RBD PA-A2-CTB chimera, which efficiently enters cells by binding to the cholera toxin receptor, elicits a total IgG antibody response comparable to that of wild-type PA; however, the toxin neutralizing antibody response elicited by this protein is much lower than that elicited by wild-type PA, suggesting that the neutralizing antibody response to PA depends on the uptake system used for entry.

DISCUSSION

In this study, we demonstrate that the receptor binding pathway of PA plays a critical role in the generation of a robust primary neutralizing antibody response. We found that receptor binding-competent wild-type PA elicited robust total anti-PA IgG

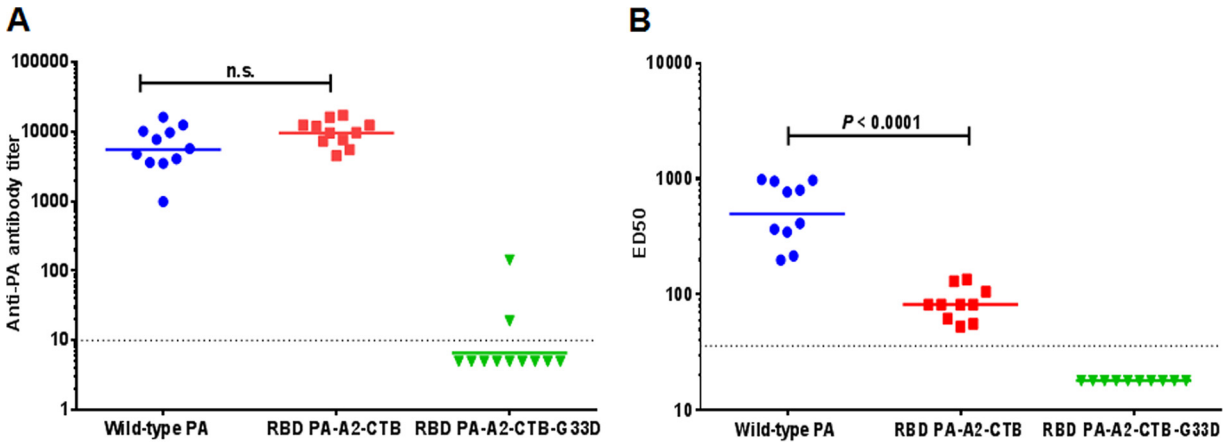

FIG 6 Antibody titers of mice immunized with wild-type PA or RBD PA-A2-CTB chimera. Groups of 10 mice each were immunized with either wild-type PA (15 μg of antigen/mouse), RBD PA-A2-CTB chimera (26 μg of antigen/mouse), or RBD PA-A2-CTB(G33D) (26 μg of antigen/mouse). The doses of antigens administered were adjusted so that equimolar amounts of wild-type PA and the chimeric proteins were administered to the mice. Twenty-eight days postimmunization, the mice were bled, and serum samples were analyzed by ELISA or the toxin neutralizing antibody assay as described in Materials and Methods. (A) Anti-PA IgG antibody titer for each mouse as determined by ELISA. (B) Toxin neutralizing antibody titer (expressed as ED_{50}) for each mouse. Each symbol represents the value for an individual mouse. The horizontal line represents the geometric mean for the group of mice. The dotted line represents the limit of quantitation of the assay. Statistical significance of differences in the responses to wild-type PA and RBD PA-A2-CTB was determined using an unpaired *t* test. The *P* value is indicated. This figure shows the results of one experiment and is representative of three independent immunization experiments. n.s., not significant.

and toxin neutralizing antibody responses; however, the RBD mutant PA that was severely impaired in its ability to bind to the PA receptor exhibited barely detected antibody responses. Previously, Yan et al. (23) examined the immunogenicity of wild-type PA and the RBD mutant PA, but they did not report the dramatic differences that we observed in our study. The discrepancy between their results and ours might be due to several factors, including the following. (i) They examined the antibody response after multiple immunizations, which would blunt differences. (ii) They reported neutralizing antibody titers from pooled sera rather than from individual mice. (iii) They adsorbed their antigens to aluminum hydroxide adjuvant, which we have found lessens differences between the IgG response elicited by wild-type PA and that elicited by the RBD mutant PA (A. Verma and D. L. Burns, unpublished results), possibly by affecting the ability of wild-type PA to bind to its receptor.

We found that uptake of wild-type PA and the RBD mutant PA which cannot bind to receptor occurs by distinctly different mechanisms. Wild-type PA uptake by DC 2.4 cells occurs by receptor-mediated endocytosis, whereas RBD mutant PA uptake occurs by fluid-phase macropinocytosis. Efficiency of uptake of wild-type PA and the RBD mutant PA by DC 2.4 cells differed dramatically. These results suggest that differences in uptake efficiency and/or the uptake pathway play a role in the differences in antibody response that we observed to the two PA proteins.

In order to investigate the relative contributions of uptake pathway and uptake efficiency to the antibody response to PA, we examined the immunogenicity of the chimeric protein RBD PA-A2-CTB, which enters the APC model cell types that we examined even more efficiently than wild-type PA does but which is taken up by cells through the cholera toxin binding pathway rather than the PA binding pathway. When the total IgG antibody response elicited by the RBD PA-A2-CTB chimera was compared to that of wild-type PA, we observed that the RBD PA-A2-CTB chimera and wild-type PA elicited similar total IgG antibody responses. However, a different picture emerged when toxin neutralizing antibody responses were compared. The neutralizing antibody response elicited by the RBD PA-A2-CTB chimera was much lower than that elicited by wild-type PA. In three independent experimental replicates, the geometric mean titer of the toxin neutralizing antibody response to the RBD PA-A2-CTB chimera ranged from 7 to 10 times lower than that elicited by wild-type PA. These results suggest that the

subcellular system by APCs to capture the antigen appears to play a critical role in development of the toxin neutralizing antibody response to PA.

Importantly, these results demonstrate that the relative magnitudes of the total IgG and toxin neutralizing antibody responses can differ depending on the capture/uptake pathway of the antigen. The total anti-PA IgG response, which was comparable for the PA and cholera toxin binding pathways, would consist of antibodies that bind to native surface epitopes as well as to epitopes that are not necessarily exposed in the native protein. (Note that antibodies to epitopes that are not exposed in the native protein can be detected by ELISA because the capture antigen used in the assay can lose some structural integrity upon adsorption to the ELISA plate [24, 25].) The finding that both binding pathways lead to a robust total anti-PA IgG antibody response suggests that both binding pathways allow efficient uptake and processing of the antigen by APCs and loading of processed peptides onto MHC for presentation to T cells. While both pathways lead to robust total anti-PA IgG responses (consisting of both functional and nonfunctional antibodies), only the PA binding pathway leads to a robust toxin neutralizing antibody response. Since neutralizing antibodies must be capable of binding to and inactivating the native form of PA, more conformationally intact antigen may be available for presentation to B cells if antigen uptake occurs via the PA receptor pathway rather than the cholera toxin receptor pathway.

The question of how unprocessed antigen might be presented to naive B cells remains an enigma. APCs might directly present intact antigen that is deposited on their cell surface to B cells (26), or APCs might retain intracellular pools of unprocessed antigen that are periodically recycled to the plasma membrane for presentation to B cells (3, 27). While a detailed picture of the presentation of conformationally intact antigen by APCs to B cells for induction of neutralizing antibodies remains obscure, the binding and internalization pathways of PA and cholera toxin differ in a number of ways that might account for the differences in neutralizing antibody response elicited by wild-type PA and the RBD PA-A2-CTB chimera protein. The possibilities include the following. (i) Retention of PA on the APC surface may be prolonged when it is bound to the PA receptor, increasing the time that the antigen is accessible to B cells. In this regard, Beauregard and colleagues found that PA is only relatively slowly internalized in comparison to other cell receptor ligands such as transferrin (28). (ii) PA structure may be stabilized by binding to its own receptor, which might result in prolonged retention of the native structure of the protein until it can be presented to B cells. In support of this possibility, others have shown that binding of PA to its major receptor, CMG2, will stabilize the protein (29). (iii) Because the PA and cholera toxin intracellular trafficking patterns differ (4, 5, 8, 19, 20), differences in trafficking pathways of PA and the RBD PA-A2-CTB chimera protein could result in differential processing of the antigen or recycling of the antigen to the cell surface. (iv) PA receptors, but not cholera toxin receptors, may be present on the specific cell type(s) responsible for presentation of unprocessed, conformationally intact antigen to B cells. While this possibility is somewhat remote, since ganglioside GM_1, the receptor for cholera toxin, is ubiquitously expressed (30), the possibility cannot be discounted entirely. It is noteworthy that if this were the case, PA and the chimera could possibly be used as tools to identify this important cell type. (v) Binding of PA to its receptor might stimulate a signaling pathway that determines the functionality of the antibody response.

While the specific facets of the antigen capture pathway of PA that are responsible for generation of an optimal neutralizing antibody response to PA remain to be determined, the results of this study provide evidence that the PA-specific binding pathway leads to a more robust antibody response than the nonspecific, low-efficiency macropinocytosis entry pathway utilized by the RBD mutant PA. The PA-specific entry pathway also leads to a more robust toxin neutralizing antibody response than does another specific capture pathway, the cholera toxin pathway, even though the total anti-PA IgG response is similar for the two pathways. Importantly, these results demonstrate that features of antigen uptake pathways that lead to a strong neutralizing

antibody response may differ from those that are important for induction of a robust total IgG antibody response.

To our knowledge, our results are the first to demonstrate that antigen capture pathways dictate the robustness of the neutralizing antibody response to a bacterial toxin as well as the ratio of neutralizing antibody to total IgG antibody response. Moreover, our results suggest that PA and, possibly, the binding components of other bacterial toxins that have well-defined uptake pathways, could be useful tools for elucidating the specific aspects of antigen capture/uptake pathways necessary for induction of optimal neutralizing antibody responses. Bacterial toxins have long been used as tools for deciphering mammalian signal transduction pathways. These results suggest that the binding components of bacterial toxins might also be important tools for delineating immune response pathways.

MATERIALS AND METHODS

Bacillus anthracis recombinant PA83 (NR-140), recombinant lethal factor (LF) (NR-142), anti-recombinant protective antigen (anti-rPA) rabbit reference polyclonal serum (NR-3839), and murine macrophage-like J774A.1 cells (NR-28) were from the NIH Biodefense and Emerging Infections Research Resources Repository, NIAID, NIH (Bethesda, MD). DC 2.4 cells were obtained from Kenneth L. Rock (Department of Pathology, University of Massachusetts Medical School). Cell culture reagents were obtained from Invitrogen (Carlsbad, CA). Pierce *N*-hydroxysuccinimide (NHS)-activated magnetic beads labeled with DyLight 488 and DyLight 594 were obtained from Thermo Scientific (Rockford, IL). Chlorpromazine hydrochloride and rottlerin were obtained from Sigma-Aldrich (St. Louis, MO).

Cloning and expression of wild-type PA gene and other mutant PA genes. Genes encoding wild-type protective antigen (PA) and receptor binding-deficient (RBD) mutant PA (N682A and D683A) were generated using *in vitro* mutagenesis and cloned in pET-22b(+) plasmid carrying an N-terminal *pelB* signal sequence for periplasmic localization. The different PA constructs were expressed and purified in *E. coli* BL21(DE3) or *E. coli* BL21 carrying plyS essentially as previously described (31). Briefly, *E. coli* cultures containing recombinant plasmid constructs were grown at 37°C in LB broth containing 100 μg/ml of ampicillin. Protein expression was induced with 1 mM isopropyl-β-D-thiogalactopyranoside (IPTG) at 30°C. Bacterial cells were harvested and resuspended in a solution of 20 mM Tris-HCl and 1 mM EDTA (pH 8.0) containing 20% sucrose and centrifuged. After centrifugation, cell pellets were resuspended in 20 mM Tris-HCl (pH 8.0) containing 5 mM $MgSO_4$ to release the periplasmic content. Wild-type PA and RBD mutant PA present in the periplasmic content were then further purified using anion-exchange and size exclusion chromatography. Purified PA proteins obtained using this procedure were approximately 95 to 99% pure as determined by sodium dodecyl sulfate-polyacrylamide gel electrophoresis (SDS-PAGE).

Construction, expression, and purification of RBD PA-A2-CTB and RBD PA-A2-CTB(G33D) mutant chimeras. The gene for RBD mutant PA was PCR amplified using forward (TTATGGCCACAGAA GTTAAACAGGAGAACCG) and reverse primers (ATTGCGGCCGCTCCTATCTCATAGCCTTTTTTAG) which contained MscI and NotI sites, respectively (restriction sites underlined). The expression plasmid used for *pag*(*RBD*) amplicon insertion was pGAP22, which is a derivative of a previously published dual-promoter expression plasmid pGAP22A2 (22). Both pGAP22 and pGAP22A2 are identical except pGAP22 contains a shortened *a2* domain that begins at amino acid 211 (Leu) of the cholera toxin A subunit (32). Insertion of *pag*(*RBD*) into the MscI and NotI restriction sites of pGAP22 sandwiched it in frame between the *pelB* signal sequence and the shortened *a2* domain. The resultant plasmid, pGAP22-RBD mutant PA, contained *pag*(*RBD*)-*a2* and *ctb* under the control of IPTG- and arabinose-inducible promoters, respectively (22). The GM_1 ganglioside binding-deficient mutation, CTBG33D, was created by site-directed mutagenesis using a QuikChange Lightning site-directed mutagenesis kit (Agilent Technologies; Santa Clara, CA) following the manufacturer's protocol. The double nucleotide mutation was created using the forward primer (CGTATACAGAATCTCTAGCTGATAAAAGAGAGATGGCTATC) and reverse primer (GATAGCCATCTC TCTTTTATCAGCTAGAGATTCTGTATACG; mutations are underlined), creating the plasmid pGAP22-RBD mutant PA-CTBG33D.

Both RBD PA-A2-CTB and RBD PA-A2-CTBG33D chimeras were expressed in *E. coli* BL21(DE3) cells and purified under the same conditions. For protein expression, cultures were grown in 500 ml of NZTCYM (1% NZ-amine, 1% tryptone, 0.5% NaCl, 0.5% yeast extract, 0.1% Casamino acids, 0.2% $MgSO_4$) (pH 7.5) with 50 μg/ml of kanamycin. The cultures were grown at 37°C with shaking at 250 rpm until they reached an optical density at 600 nm of ~3.0. The incubation temperature was then reduced to 16°C, and the cultures were incubated for 30 to 60 min with shaking at 250 rpm to acclimate to the new temperature. The cultures were then induced with 0.1 mM IPTG and 0.1% arabinose for 16 to 18 h at 16°C and 250 rpm. Following induction, cell pellets were harvested by centrifugation and stored at −80°C until use.

For purification, cell pellets were thawed and suspended in phosphate buffer (50 mM NaH_2PO_4 plus 300 mM NaCl [pH 8.0]). Soluble extracts were obtained by adding Elugent detergent to a final concentration of 2% to the suspension, followed by rLysozyme and Benzonase (following the manufacturer's recommendations; EMD Millipore, Billerica, MA). The cell extracts were mixed at room temperature for 15 to 30 min until no longer viscous. The cell extracts were then clarified by centrifugation for 10 min at 20,200 × *g* and 4°C. Talon metal affinity resin (Clontech, Mountain View, CA) was added to the clarified extract and incubated with mixing at room temperature for 30 min. The resin was then added to a

column and washed with 75 bed volumes of the above phosphate buffer. The chimeras were eluted from the resin using imidazole elution buffer (50 mM NaH_2PO_4 plus 300 mM NaCl and 250 mM imidazole [pH 8.0]). CTB or CTBG33D monomers were separated from the chimera using size exclusion chromatography. Purified chimeras were more than 95% pure as determined by SDS-PAGE and were stored at −70°C.

Internalization assays using dendritic cells. *In vitro* internalization assays with wild-type PA and other PA mutants proteins were performed at 37°C using DC 2.4 cells. DC 2.4 cells were grown in six-well plates to 90% confluence. DC 2.4 cells were incubated with PA proteins for 90 min at 37°C. For internalization inhibition studies, DC 2.4 cells were pretreated either with chlorpromazine (50 μM) or rottlerin (5 μM) for 30 min before the addition of PA proteins. After pretreatment, PA proteins were added, and further incubation was continued at 37°C for 90 min in the presence of inhibitors. After incubation, DC 2.4 cells were washed three times with phosphate-buffered saline (PBS), treated for 5 min with low-pH buffer (50 mM glycine and 100 mM NaCl, pH 4.0) to remove the PA proteins bound to the cell surface and again washed three times with PBS. The DC 2.4 cells were lysed with mammalian protein extraction reagent (MPER) lysis buffer (Pierce) containing 1× Halt protease inhibitor cocktail and 10 U of DNase/ml. The cell lysates (30 μg of total protein) were subjected to SDS-PAGE analysis using 4 to 20% Tris-glycine gradient gels (Novex, San Diego). Proteins were then transferred to nitrocellulose membranes, followed by Western blotting using anti-PA antibodies.

Labeling of PA proteins, confocal microscopy, and image processing. Wild-type PA and RBD mutant PA were conjugated with DyLight 488 and DyLight 594 following the manufacturer's instructions (Thermo Scientific, Rockford, IL). Conjugation ratios were calculated based on absorbance of the conjugates at their respective wavelengths and the molar extinction coefficient for the specific DyLight dye. DyLight-labeled wild-type PA and RBD mutant PA proteins with a conjugation ratio of ~1 (one fluorescent dye molecule/PA molecule) were used for confocal microscopy. DC 2.4 cells (cultured on coverslip) were incubated with wild-type PA labeled with DyLight 594 (wild-type PA-DyLight 594) and RBD mutant PA labeled with DyLight 488 (RBD mutant PA-DyLight 488) both at a concentration of 5 μg/ml and also, the RBD mutant PA-DyLight 488 at a concentration of 100 μg/ml for 30 min at 37°C. After incubation, the cells were washed three times with PBS, treated very briefly with low-pH buffer (50 mM glycine and 100 mM NaCl [pH 4.0]) and then extensively washed with PBS. Cells were fixed using 4% paraformaldehyde and mounted onto slide using a mounting medium containing 4′,6′-diamidino-2-phenylindole (DAPI) for nuclear staining. Slides were visualized using Zeiss AxioObserver, SD spinning disk confocal microscope (Carl Zeiss Microscopy LLC, Thornwood, NY). The image data were stored as zvi format for further analysis. Huygens Professional software (Scientific Volume Imaging BV, Hilversum, Netherlands) was used for deconvolution with classic maximum likelihood estimation algorithm and a theoretical point spread function. The deconvolved image data were then visualized by Imaris image visualization and analysis software (Bitplane USA, Concord, MA).

Immunization studies with wild-type PA and mutant PA proteins. Groups of 10 mice (6-week-old female CD-1 mice) were immunized once intraperitoneally with PA proteins in normal saline or PBS. Control groups of 10 mice were simultaneously immunized with normal saline or PBS. Immunizations and serum collections were carried out by Cocalico Biologicals, Inc. (Reamstown, PA) in compliance with the guidelines of their Institutional Animal Care and Use Committee. Mice were bled 28 days postimmunization. Serum samples collected from the different groups of mice were analyzed individually using the toxin neutralization antibody assay and anti-PA antibody ELISA.

Toxin neutralizing antibody assay. Sera from different immunization studies were analyzed by the toxin neutralizing antibody assay using J774A.1 cells essentially as described previously (33). Neutralization of lethal toxin cytotoxicity was measured by assessing cell viability with twofold serial dilutions of the test serum and a reference rabbit polyclonal serum (NR-3839) as described earlier (31). A four-parameter logistic regression model was used to fit the data points generated when the absorbance was plotted against the reciprocal of the serum dilution. The inflection point, which indicates 50% neutralization, was reported as the effective dilution at 50% inhibition (ED_{50}) (34), which is defined as the reciprocal of the serum dilution at 50% inhibition. For the toxin neutralizing antibody depletion analysis, wild-type PA and RBD mutant PA proteins were coupled to Pierce NHS-activated magnetic beads. After the proteins and beads were coupled, the wild-type PA- and RBD mutant PA-coupled beads were incubated with wild-type PA antisera overnight at 4°C to deplete toxin neutralizing antibodies. After overnight incubation, depleted antisera along with nondepleted antisera were analyzed by the toxin neutralizing antibody assay as described above.

Anti-PA ELISA. Total anti-PA IgG antibodies were measured by ELISA essentially as described previously (31). Briefly, the wells on microtiter plates were coated with wild-type PA (100 ng/well) in PBS, pH 7.4, overnight at 4°C. Each well was washed three times with 300 μl wash buffer (PBS [pH 7.4] with 0.05% Tween 20). Individual serum samples from different groups of immunized mice were diluted to 1:12.5 in 5% skim milk in PBS with 0.1% Tween 20 and then serially diluted fourfold in a separate plate. Diluted serum samples (100 μl) were transferred to the wells on an ELISA plate and incubated for 1 h at 37°C. After incubation, the wells were washed, and 100 μl of horseradish peroxidase-labeled anti-mouse IgG (H+L) (KPL, Gaithersburg, MD) was added to each well at a 1:4,000 dilution. After 1 h of incubation at 37°C, the wells were washed, and 100 μl of 2,2′-azinobis(3-ethylbenthiazolinesulfonic acid) (ABTS) peroxidase substrate (KPL, Gaithersburg, MD) was added to each well and incubated for 30 min at 37°C. Color development was stopped by the addition of ABTS stop solution. Absorbance at 405 nm was measured. A four-parameter logistic regression model was used to fit the data points generated when the optical density was plotted against the reciprocal of the serum dilution. The inflection point of the curve, which indicates 50% response, was reported as the antibody titer.

Statistical analyses. Statistical analyses were performed using GraphPad Prism software (version 6; GraphPad Prism Software, Inc., La Jolla, CA). For the toxin neutralizing antibody assay, all nonresponder mice were assigned an ED_{50} value of 18 (1/2 the limit of quantitation of the toxin neutralizing antibody assay). For the ELISA, all nonresponder mice were assigned an antibody titer value of 5 (1/2 the limit of quantitation of the ELISA).

ACKNOWLEDGMENTS

The following reagents were obtained from the NIH Biodefense and Emerging Infections Research Resources Repository, NIAID, NIH: recombinant PA83 (NR-140) from *B. anthracis*, recombinant LF (NR-142) from *B. anthracis*, anti-rPA rabbit reference polyclonal serum pool (NR-3839), and murine macrophage-like J774A.1 cells (NR-28). DC 2.4 cells were obtained from Kenneth L. Rock (Department of Pathology, University of Massachusetts Medical School).

This work was funded by the Food and Drug Administration Intramural Research Program.

The funders had no role in study design, data collection and interpretation, or the decision to submit the work for publication.

REFERENCES

1. Siegrist CA. 2008. Vaccine immunology, p 17–36. *In* Plotkin SA, Orenstein WA, Offit PA (ed), Vaccines, 5th ed. Saunders/Elsevier, Philadelphia, PA.
2. Heesters BA, Chatterjee P, Kim YA, Gonzalez SF, Kuligowski MP, Kirchhausen T, Carroll MC. 2013. Endocytosis and recycling of immune complexes by follicular dendritic cells enhances B cell antigen binding and activation. Immunity 38:1164–1175. https://doi.org/10.1016/j.immuni.2013.02.023.
3. Bergtold A, Desai DD, Gavhane A, Clynes R. 2005. Cell surface recycling of internalized antigen permits dendritic cell priming of B cells. Immunity 23:503–514. https://doi.org/10.1016/j.immuni.2005.09.013.
4. Friebe S, van der Goot FG, Bürgi J. 2016. The ins and outs of anthrax toxin. Toxins 8:69. https://doi.org/10.3390/toxins8030069.
5. Collier RJ, Young JA. 2003. Anthrax toxin. Annu Rev Cell Dev Biol 19:45–70. https://doi.org/10.1146/annurev.cellbio.19.111301.140655.
6. Liu S, Crown D, Miller-Randolph S, Moayeri M, Wang H, Hu H, Morley T, Leppla SH. 2009. Capillary morphogenesis protein-2 is the major receptor mediating lethality of anthrax toxin in vivo. Proc Natl Acad Sci U S A 106:12424–12429. https://doi.org/10.1073/pnas.0905409106.
7. Young JA, Collier RJ. 2007. Anthrax toxin: receptor binding, internalization, pore formation, and translocation. Annu Rev Biochem 76:243–265. https://doi.org/10.1146/annurev.biochem.75.103004.142728.
8. Abrami L, Lindsay M, Parton RG, Leppla SH, van der Goot FG. 2004. Membrane insertion of anthrax protective antigen and cytoplasmic delivery of lethal factor occur at different stages of the endocytic pathway. J Cell Biol 166:645–651. https://doi.org/10.1083/jcb.200312072.
9. Ionin B, Hopkins RJ, Pleune B, Sivko GS, Reid FM, Clement KH, Rudge TL, Jr, Stark GV, Innes A, Sari S, Guina T, Howard C, Smith J, Swoboda ML, Vert-Wong E, Johnson V, Nabors GS, Skiadopoulos MH. 2013. Evaluation of immunogenicity and efficacy of anthrax vaccine adsorbed for post-exposure prophylaxis. Clin Vaccine Immunol 20:1016–1026. https://doi.org/10.1128/CVI.00099-13.
10. Pitt ML, Little SF, Ivins BE, Fellows P, Barth J, Hewetson J, Gibbs P, Dertzbaugh M, Friedlander AM. 2001. In vitro correlate of immunity in a rabbit model of inhalational anthrax. Vaccine 19:4768–4773. https://doi.org/10.1016/S0264-410X(01)00234-1.
11. Chen L, Schiffer JM, Dalton S, Sabourin CL, Niemuth NA, Plikaytis BD, Quinn CP. 2014. Comprehensive analysis and selection of anthrax vaccine adsorbed immune correlates of protection in rhesus macaques. Clin Vaccine Immunol 21:1512–1520. https://doi.org/10.1128/CVI.00469-14.
12. Verma A, McNichol B, Domínguez-Castillo RI, Amador-Molina JC, Arciniega JL, Reiter K, Meade BD, Ngundi MM, Stibitz S, Burns DL. 2013. Use of site-directed mutagenesis to model the effects of spontaneous deamidation on the immunogenicity of Bacillus anthracis protective antigen. Infect Immun 81:278–284. https://doi.org/10.1128/IAI.00863-12.
13. Zomber G, Reuveny S, Garti N, Shafferman A, Elhanany E. 2005. Effects of spontaneous deamidation on the cytotoxic activity of the Bacillus anthracis protective antigen. J Biol Chem 280:39897–39906. https://doi.org/10.1074/jbc.M508569200.
14. Rosovitz MJ, Schuck P, Varughese M, Chopra AP, Mehra V, Singh Y, McGinnis LM, Leppla SH. 2003. Alanine-scanning mutations in domain 4 of anthrax toxin protective antigen reveal residues important for binding to the cellular receptor and to a neutralizing monoclonal antibody. J Biol Chem 278:30936–30944. https://doi.org/10.1074/jbc.M301154200.
15. Singh Y, Klimpel KR, Quinn CP, Chaudhary VK, Leppla SH. 1991. The carboxyl-terminal end of protective antigen is required for receptor binding and anthrax toxin activity. J Biol Chem 266:15493–15497.
16. Novak JM, Stein MP, Little SF, Leppla SH, Friedlander AM. 1992. Functional characterization of protease-treated Bacillus anthracis protective antigen. J Biol Chem 267:17186–17193.
17. Wang LH, Rothberg KG, Anderson RG. 1993. Mis-assembly of clathrin lattices on endosomes reveals a regulatory switch for coated pit formation. J Cell Biol 123:1107–1117. https://doi.org/10.1083/jcb.123.5.1107.
18. Sarkar K, Kruhlak MJ, Erlandsen SL, Shaw S. 2005. Selective inhibition by rottlerin of macropinocytosis in monocyte-derived dendritic cells. Immunology 116:513–524. https://doi.org/10.1111/j.1365-2567.2005.02253.x.
19. Wernick NL, Chinnapen DJ, Cho JA, Lencer WI. 2010. Cholera toxin: an intracellular journey into the cytosol by way of the endoplasmic reticulum. Toxins 2:310–325. https://doi.org/10.3390/toxins2030310.
20. Lencer WI. 2004. Retrograde transport of cholera toxin into the ER of host cells. Int J Med Microbiol 293:491–494. https://doi.org/10.1078/1438-4221-00293.
21. Jobling MG, Holmes RK. 1991. Analysis of structure and function of the B subunit of cholera toxin by the use of site-directed mutagenesis. Mol Microbiol 5:1755–1767. https://doi.org/10.1111/j.1365-2958.1991.tb01925.x.
22. Price GA, Holmes RK. 2012. Evaluation of TcpF-A2-CTB chimera and evidence of additive protective efficacy of immunizing with TcpF and CTB in the suckling mouse model of cholera. PLoS One 7:e42434. https://doi.org/10.1371/journal.pone.0042434.
23. Yan M, Roehrl MH, Basar E, Wang JY. 2008. Selection and evaluation of the immunogenicity of protective antigen mutants as anthrax vaccine candidates. Vaccine 26:947–955. https://doi.org/10.1016/j.vaccine.2007.11.087.
24. Holm BE, Bergmann AC, Hansen PR, Koch C, Houen G, Trier NH. 2015. Antibodies with specificity for native and denatured forms of ovalbumin differ in reactivity between enzyme-linked immunosorbent assays. APMIS 123:136–145. https://doi.org/10.1111/apm.12329.
25. Kilshaw PJ, McEwan FJ, Baker KC, Cant AJ. 1986. Studies on the specificity of antibodies to ovalbumin in normal human serum: technical considerations in the use of ELISA methods. Clin Exp Immunol 66:481–489.
26. Batista FD, Harwood NE. 2009. The who, how and where of antigen presentation to B cells. Nat Rev Immunol 9:15–27. https://doi.org/10.1038/nri2454.
27. Qi H, Egen JG, Huang AY, Germain RN. 2006. Extrafollicular activation of lymph node B cells by antigen-bearing dendritic cells. Science 312:1672–1676. https://doi.org/10.1126/science.1125703.
28. Beauregard KE, Collier RJ, Swanson JA. 2000. Proteolytic activation of receptor-bound anthrax protective antigen on macrophages promotes

its internalization. Cell Microbiol 2:251–258. https://doi.org/10.1046/j.1462-5822.2000.00052.x.
29. Mullangi V, Mamillapalli S, Anderson DJ, Bann JG, Miyagi M. 2014. Long-range stabilization of anthrax protective antigen upon binding to CMG2. Biochemistry 53:6084–6091. https://doi.org/10.1021/bi500718g.
30. Eidels L, Proia RL, Hart DA. 1983. Membrane receptors for bacterial toxins. Microbiol Rev 47:596–620.
31. Wagner L, Verma A, Meade BD, Reiter K, Narum DL, Brady RA, Little SF, Burns DL. 2012. Structural and immunological analysis of anthrax recombinant protective antigen adsorbed to aluminum hydroxide adjuvant. Clin Vaccine Immunol 19:1465–1473. https://doi.org/10.1128/CVI.00174-12.
32. Zhang RG, Scott DL, Westbrook ML, Nance S, Spangler BD, Shipley GG, Westbrook EM. 1995. The three-dimensional crystal structure of cholera toxin. J Mol Biol 251:563–573. https://doi.org/10.1006/jmbi.1995.0456.
33. Omland KS, Brys A, Lansky D, Clement K, Lynn F, Participating Laboratories. 2008. Interlaboratory comparison of results of an anthrax lethal toxin neutralization assay for assessment of functional antibodies in multiple species. Clin Vaccine Immunol 15:946–953. https://doi.org/10.1128/CVI.00003-08.
34. Ngundi MM, Meade BD, Lin TL, Tang WJ, Burns DL. 2010. Comparison of three anthrax toxin neutralization assays. Clin Vaccine Immunol 17:895–903. https://doi.org/10.1128/CVI.00513-09.